

pubs.acs.org/acschemicalbiology Articles

In Vitro Reconstitution of Fimsbactin Biosynthesis from Acinetobacter baumannii

Jinping Yang and Timothy A. Wencewicz*



Cite This: https://doi.org/10.1021/acschembio.2c00573



ACCESS I

III Metrics & More

Article Recommendations

s Supporting Information

ABSTRACT: Siderophores produced via nonribosomal peptide synthetase (NRPS) pathways serve as critical virulence factors for many pathogenic bacteria. Improved knowledge of siderophore biosynthesis guides the development of inhibitors, vaccines, and other therapeutic strategies. Fimsbactin A is a mixed ligand siderophore derived from human pathogenic *Acinetobacter baumannii* that contains phenolate—oxazoline, catechol, and hydroxamate metal chelating groups branching from a central L-Ser tetrahedral unit via amide and ester linkages. Fimsbactin A is derived from two molecules of L-Ser, two molecules of 2,3-dihydroxybenzoic acid (DHB), and one molecule of L-Orn and is a product of the *fbs* biosynthetic operon. Here, we report the

Acinetobacter baumannii ATCC 17978

fbs A B D B F G H J J D LM N D P Q

2,3-DHB loading FbsH FbsE FbsF FbsG FbsJK

A T Cy A T C A T C H₂N D H₂N D

complete *in vitro* reconstitution of fimsbactin A biosynthesis in a cell-free system using purified enzymes. We demonstrate the conversion of L-Orn to N_1 -acetyl- N_1 -hydroxy-putrescine (ahPutr) via ordered action of FbsJ (decarboxylase), FbsI (flavin N_1 -monoxygenase), and FbsK (N_1 -acetyltransferase). We achieve conversion of L-Ser, DHB, and L-Orn to fimsbactin A using FbsIJK in combination with the NRPS modules FbsEFGH. We also demonstrate chemoenzymatic conversion of synthetic ahPutr to fimsbactin A using FbsEFGH and establish the substrate selectivity for the NRPS adenylation domains in FbsH (DHB) and FbsF (L-Ser). We assign a role for the type II thioesterase FbsM in producing the shunt metabolite 2-(2,3-dihydroxyphenyl)-4,5-dihydroxazole-4-carboxylic acid (DHB-oxa) via cleavage of the corresponding thioester intermediate that is tethered to NRPS peptidyl carrier domains during biosynthetic assembly. We propose a mechanism for branching NRPS-derived peptides via amide and ester linkages via the dynamic equilibration of N-DHB-Ser and O-DHB-Ser thioester intermediates via hydrolysis of DHB-oxa thioester intermediates. We also propose a genetic signature for NRPS "branching" in the presence of a terminating C-T-C motif (FbsG).

■ INTRODUCTION

Siderophores are conditionally essential secondary metabolites produced by bacteria for iron acquisition. Siderophore scaffolds present oxo-ligands (catechols, phenolateoxazolines, hydroxamates, and α-hydroxy-carboxylates) to enable the formation of high-affinity octahedral ferric complexes. Most siderophores are peptide-based structures assembled via two primary biosynthetic enzyme types: (1) nonribosomal peptide synthetases (NRPSs); (2) NRPS-independent siderophore (NISs) synthetases. NRPS and NIS siderophore biosynthetic pathways have been targeted for inhibition by small molecules and antibodies as antivirulence agents. Detailed characterization of siderophore biosynthesis and utilization in target pathogens is needed to guide the development of inhibitors, vaccines, and drug delivery systems as therapeutic strategies.

Our group is developing siderophore-based therapeutics against the multi-drug resistant (MDR) Gram-negative human pathogen *Acinetobacter baumannii*. Strains of human pathogenic *A. baumannii* produce up to three siderophores, including NRPS-derived pre-acinetobactin and fimsbactin A (Figure 1) and NIS-derived baumannoferrin. Pre-acinetobactin and fimsbactin A are structurally related through the

presence of a phenolate—oxazoline derived from 2,3-dihydroxybenzoic acid (DHB) and L-Thr or L-Ser, respectively. The phenolate—oxazoline in pre-acinetobactin also contains one molecule of histamine joined via a N-hydroxyamide linkage. Pre-acinetobactin undergoes a nonenzymatic isomerization from the oxazoline form to an isooxazolidinone (acinetobactin), where both isomers play a role in iron acquisition. Acinetobactin production in human pathogenic A. baumannii is strictly conserved and is essential for virulence, while fimsbactin biosynthesis and transport loci only appear in ~2% of sequenced A. baumannii isolates, and the disruption of fimsbactin pathway only mildly attenuates bacterial survival and proliferation within the host. 12 Nevertheless, fimsbactin A can outcompete acinetobactin for uptake due in part to its

Received: July 13, 2022 Accepted: September 6, 2022



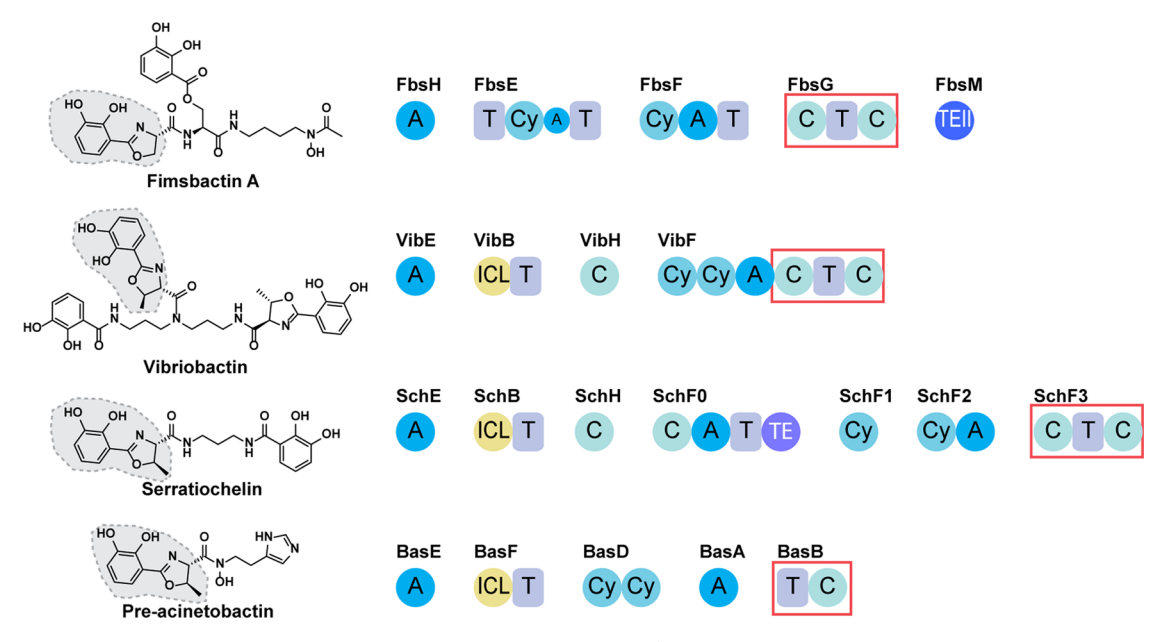


Figure 1. Chemical structures of phenolate—oxazoline-containing siderophores (fimsbactin A, vibriobactin, serratiochelin, and pre-acinetobactin) and associated NRPS assembly line domains and modules. The terminating NRPS module for each pathway is highlighted with a red box.

Figure 2. Fimsbactin siderophores A-F produced by the fbs operons present in A. baumannii and Acinetobacter baylyi with retrobiosynthetic analysis of the major analogue, fimsbactin A.

ability to form 1:1 ferric complexes that are more thermodynamically and kinetically stable than acinetobactin/pre-acinetobactin, which form 2:1 ferric complexes. ^{13,14} These properties make fimsbactin A an attractive candidate for siderophore-based antivirulence therapeutics targeting *A. baumannii* iron acquisition pathways.

Six analogues of fimsbactin (A–F) have been reported, with fimsbactin A representing the major compound isolated from fermentations (Figure 2).¹⁵ Fimsbactin A is derived from two molecules of L-Ser, two molecules of DHB, and one molecule of L-Orn. The mixed ligand fimsbactin scaffold contains phenolate—oxazoline, catechol, and hydroxamate metal chelat-

ing groups that branch from the α -carbon of a central L-Ser unit. The phenolate—oxazoline moiety originates from condensation of DHB with L-Ser, where the 2-(2,3-dihydroxyphenyl)-4,5-dihydroxazole-4-carboxylic acid (DHB-oxa) is in amide linkage with the α -amino group of the central L-Ser unit. The β -hydroxyl group of the central L-Ser unit is joined via an ester linkage to a second molecule of DHB, while the α -carboxyl group is joined via amide linkage with the N_6 primary amine of N_1 -acetyl- N_1 -hydroxy-putrescine (ahPutr). The branched peptide scaffold featuring both N- and O-acylation of L-Ser represents a new mechanistic puzzle for biosynthetic peptide assembly by NRPS modules.

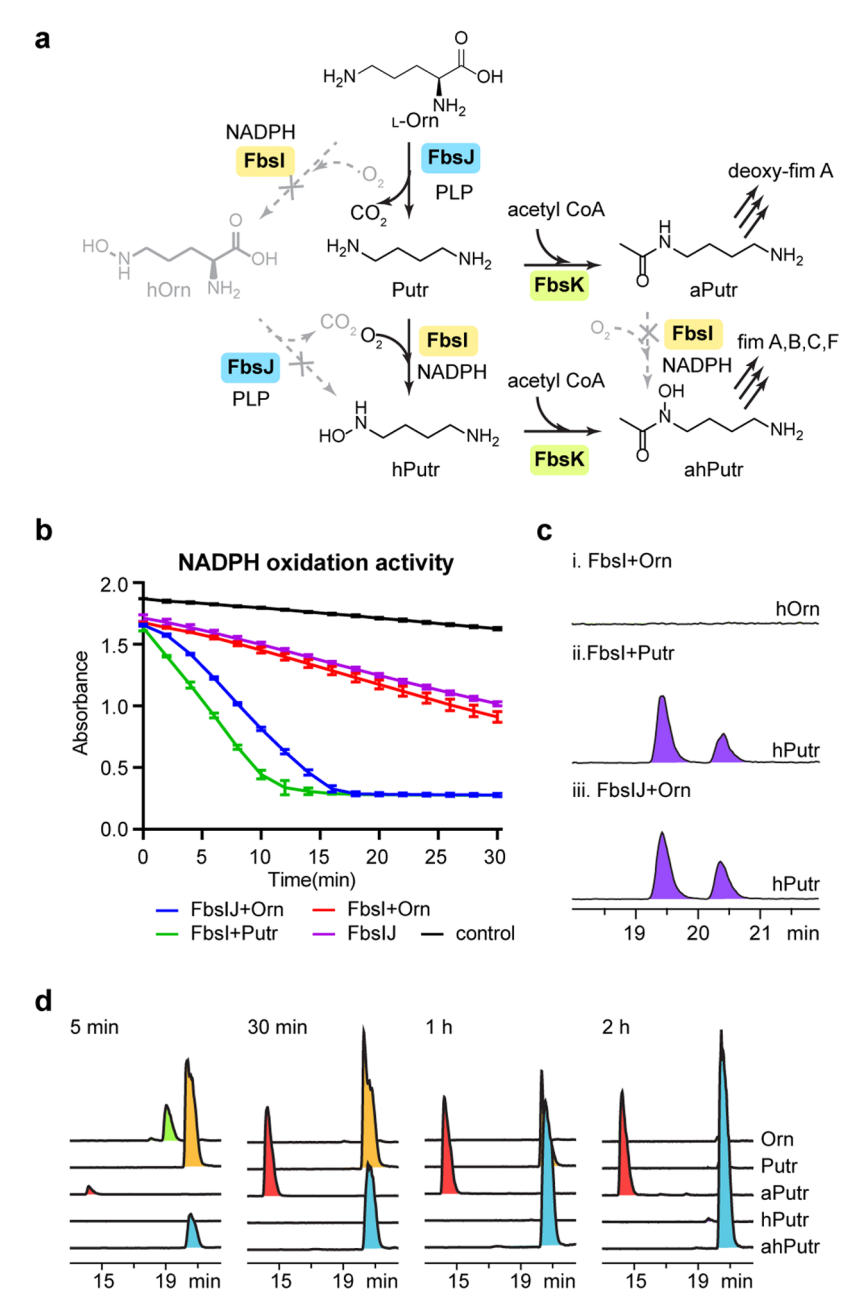


Figure 3. In vitro reconstitution of FbsI (L-Orn decarboxylase), FbsJ (putrescine N-monooxygenase), and FbsK (N-hydroxy-putrescine N-acetyltransferase) activity confirms substrates and timing for enzymatic conversion of L-Orn to ahPutr. (a) Reaction scheme depicting the observed (solid arrows) and unobserved possible routes (dashed arrows) from L-Orn to ahPutr. (b) Optical absorbance monitored at 340 nm over time and (c) EIC chromatograms for expected [M + H]⁺ molecular ions corresponding to products hOrn and hPutr from liquid chromatography—mass spectrometry (LC—MS) analysis (30 min; w/Fmoc tagging) of FbsI and FbsJ individual and combined reactions using L-Orn or Putr as substrate. (d) EIC chromatograms for Orn, Putr, aPutr, hPutr, and ahPutr from LC—MS analysis (variable time; w/Fmoc tagging) of combined FbsIJK reactions starting from L-Orn with all necessary cofactors and cosubstrates. All experiments were performed in duplicate as independent trials. LC—MS EIC traces were normalized to an Fmoc-Ala-OH internal standard. Error bars represent standard deviation.

The fbsA-Q operons in A. baylyi ADP1 (environmental strain) and A. baumannii ATCC 17978 (human pathogenic strain) encode for predicted biosynthetic enzymes (FbsB-M) and utilization/transport/regulation proteins (FbsA,N,O,Q) (Figure S1 and Table S1). FbsB-D and FbsI-K are predicted to be involved in the biosynthesis of the precursor metabolites DHB and ahPutr, respectively, while FbsE-H and FbsL,M make up the NRPS assembly line (Figures 1 and 2). FbsL is a predicted phosphopantetheinyl transferase (PPTase) presumably required for priming the acyl carrier domains with the

needed phosphopantetheinyl (PPant) prosthetic thiol group. ¹⁶ FbsM is a predicted type II thioesterase (TEII) that might serve an editing, ¹⁷ shunting, ¹⁸ and/or acyl transfer function. ¹⁹ FbsH is predicted to be a standalone adenylation (A_1) domain with selectivity for DHB as the substrate. FbsE is predicted to be a four-domain elongation NRPS module that contains *N*-terminal aryl acyl carrier (T_1), cyclization (Cy_1), a truncated adenylation (A_2), and C-terminal peptidyl carrier (T_2) domains. FbsF is predicted to be a three-domain elongation module that contains *N*-terminal cyclization (Cy_2), L-Ser-

activating adenylation (A_3), and C-terminal peptidyl carrier (T_3) domains. FbsG is predicted to be a three-domain terminating module with an unusual domain architecture composed of N-terminal condensation (C_1), peptidyl carrier (T_4), and C-terminal condensation (C_2) domains. This unusual C-T-C domain orientation is observed for other siderophores, including vibriobactin and serratiochelin (Figures 1 and S2). The presence of the C-terminal C_2 -domain in FbsG suggests that final product cleavage from the FbsG- T_4 -domain is achieved via nucleophilic acyl substitution with ahPutr, similar to the N-hydroxy-histamine nucleophilic termination mechanism observed for BasB in acinetobactin, AngM in anguibactin, and PmsG in pseudomonine biosynthesis.

We sought to investigate the substrate selectivity, order, and timing of the fimsbactin NRPS assembly line modules to gain insight into the mechanistic paradigms for peptide branching via N- and O-acylation of L-Ser and substrate cleavage facilitated by a terminating C-domain that catalyzes intermolecular nucleophilic acyl substitution during product release. Hence, we developed a cell-free in vitro reconstitution of the fimsbactin biosynthetic pathway using purified enzymes. We demonstrate the conversion of L-Orn to ahPutr by the combined action of FbsIJK coupled to complete conversion to fimsbactin A via FbsEFGH-catalyzed reactions. We also assign a function for the TEII domain FbsM in generating the shunt metabolite DHB-oxa via hydrolysis of the corresponding Tdomain-tethered thioester intermediates. Finally, we propose a mechanism for N- and O-acylation of L-Ser via bifurcation of intermediate thioester-tethered oxazolines that partition DHBoxa between N-DHB-Ser and O-DHB-Ser to achieve peptide branching through amide and ester linkages.

RESULTS AND DISCUSSION

Annotation of the Fimsbactin BGC. In 2013, the Bode group first reported the structure and biosynthetic gene clusters (BGCs) for fimsbactin from A. baumannii and A. baylyi (Figure S1 and Table S1).8 The fimsbactin BGCs appeared to be highly conserved between these strains, except for apparent truncations in the fbsF and fbsH genes in A. baumannii. Our initial cloning and heterologous expression of fbsH and fbsF resulted in low expression levels, poor solubility, and a lack of adenylation activity toward DHB and L-Ser, respectively. The inclusion of N-terminal SUMO tags did little to improve expression and solubility. The genome sequence of A. baumannii ATCC 17978 was deposited in 2020 (GenBank Assembly Accession: GCA_013372085.1), and more careful annotation of the fbs operon revealed several sequencing errors in the original 2013 report (GenBank Assembly Accession: GCA 000015425.1). Sequence analysis of the A. baumannii ATCC 17978 revealed that fbsF does encode for an intact NRPS module with a N-to-C-terminal Cy-A-T domain orientation. Additionally, fbsH was shown to have an additional 20 amino acid residues at the C-terminus that contains a conserved Lys residue shown in homologous Adomains to play a key role in orienting the carboxyl group of the aryl acids to undergo the adenylation reaction.²⁵ Cloning and expression of fbsF and fbsH from A. baumannii ATCC 17978 gave high expression levels and good protein solubility from Escherichia coli BL21. This encouraged us to individually clone all fbs biosynthetic genes (fbsEFGHIJKM) into a pET28a plasmid for heterologous expression in E. coli and

subsequent *in vitro* reconstitution of enzymatic activity (Figure S3 and Tables S2–S6).

In Vitro Reconstitution of N₁-Acetyl-N₁-hydroxyputrescine (ahPutr) Biosynthesis. The fbsIJK genes are predicted to enable conversion of L-Orn to ahPutr (Figure 3a). FbsI is predicted to be a class II flavin monooxygenase (FMO). FbsJ is predicted to be a PLP-dependent decarboxylase. FbsK is predicted to be an N-acetyltransferase. Similar combinations of these three enzymes are found in many hydroxamate-containing siderophore biosynthetic pathways through the substrates, and timing of enzyme action can vary. 26,27 FbsI belongs to the SidA/IudD/PvdA family of class II FMOs known as siderophore-related N-hydroxylating monooxygenases (NMOs).²⁸ These NMOs typically catalyze the hydroxylation of the free amino group of diamino acid, typically L-Lys or L-Orn, or diamine, typically cadaverine or putrescine, substrates. The resulting N-hydroxylamine products can be further oxidized to nitroso or nitro-containing compounds²⁹ but are more typically N-acylated to generate the corresponding hydroxamic acids. 30,31

To establish the timing and preferred substrate of FbsI, we leveraged an NAD(P)H oxidation assay monitored by the continuous measurement of optical absorbance at 340 nm (Figures 3b and S4). The rate of NADPH oxidation increased significantly when Putr was used as the substrate compared to L-Orn. NADPH was strongly preferred over NADH as the cosubstrate for the Putr+FbsI reactions. The combination of NMO FbsI and decarboxylase FbsJ/PLP with L-Orn as substrate gave the same apparent rate of NADPH oxidation as FbsI with Putr as the substrate. LC-MS analysis of the FbsI and FbsJ reactions were consistent with these results showing the production of hPutr from Putr+FbsI and Orn+FbsIJ, while no hOrn was observed for the Orn+FbsI reaction (Figure 3c). The inclusion of acyltransferase FbsK and acetyl-CoA into the FbsIJ reactions resulted in the time and enzyme-dependent formation of ahPutr (Figure 3d). We used an NADPH regeneration system (G-6-P dehydrogenase, NADP+, and G-6-P) to drive the FbsIJK reaction to completion and enable a preparative enzymatic route to ahPutr (Figure S5). We also completed a chemical synthesis of ahPutr (Scheme S1) to confirm the identity of the enzymatic product and obtain enough of this precursor for the chemoenzymatic synthesis of fimsbactin A (vida infra). We observed the formation of Nacetyl-Putr (aPutr) during the FbsIJK coupled assays and confirmed that aPutr levels remain constant throughout the reactions. The formation of aPutr is consistent with the isolation of fimsbactin D, which contains N-acetyl-diaminopropane instead of ahPutr. Control reactions where FbsK and Putr are preincubated to generate aPutr did not go to completion, and aPutr concentrations remained constant after subsequent addition of FbsI. This supports that Putr, but not aPutr or Orn (vida supra), is the relevant substrate for FbsI Nhydroxylation. These results and additional control reactions (Figure S6) support the following sequence of events: (1) decarboxylation of L-Orn by FbsJ/PLP to produce Putr; (2) N_1 -hydroxylation of Putr by FbsI/NADPH/O₂ to produce hPutr; and (3) N_1 -acetylation of hPutr by FbsK/acetyl-CoA to produce ahPutr.

Sequence and Structural Comparison of Fbsl to Other Siderophore-Related NMOs. The structural features and active site residues that allow FbsI and related NMOs to distinguish between structurally related substrates such as Lys/Orn or cadaverine/Putr are not entirely understood. A recent

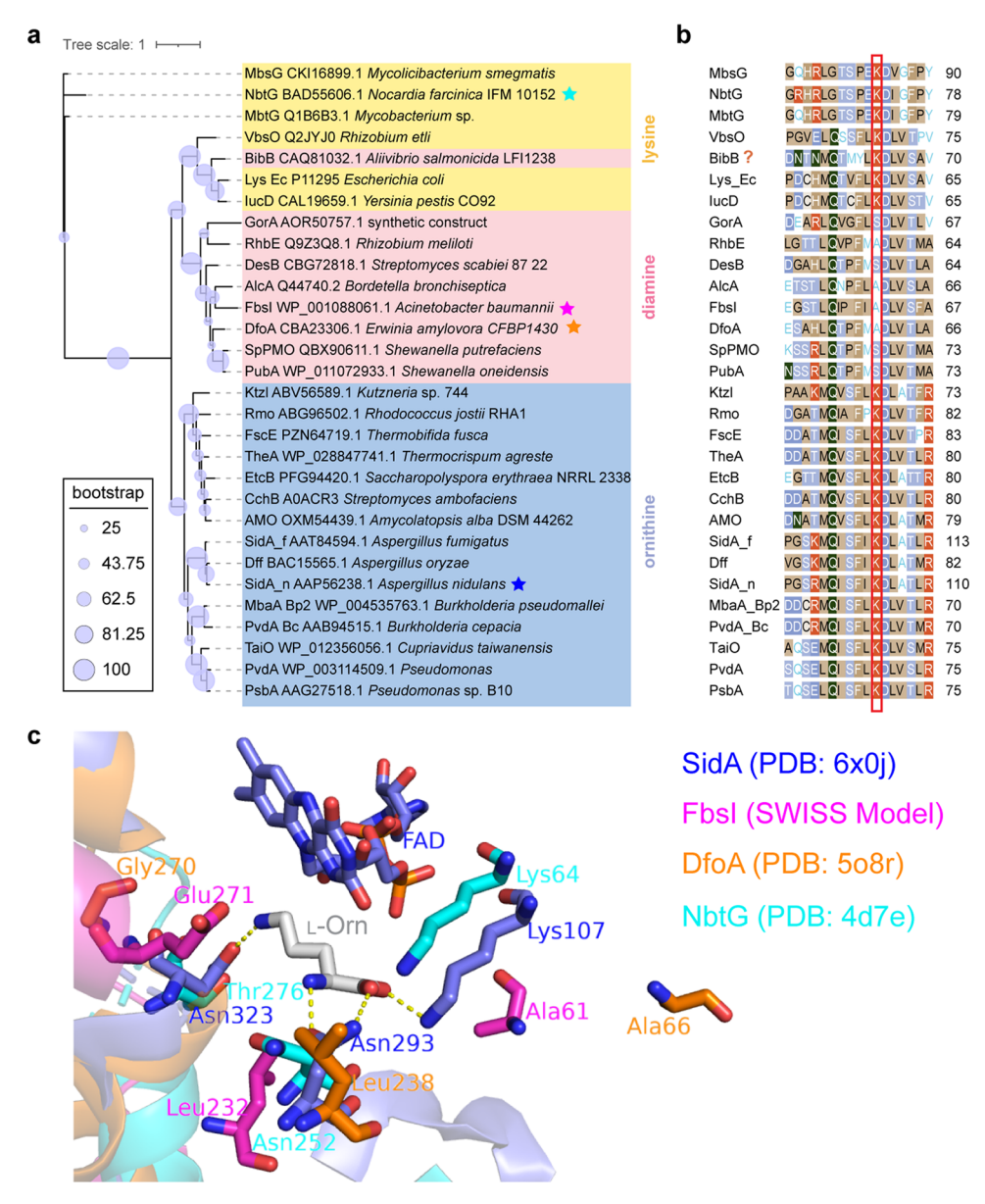


Figure 4. Phylogenetic, sequence, and structural relationships of flavin-dependent NMOs. (a) Maximum likelihood tree of 30 selected NMOs built using the "PhyML+SMS/OneClick" method available on the web: http://ngphylogeny.fr. (b) Pairwise sequence alignment of 30 selected NMOs generated using the Clustal Omega multiple sequence alignment tool available via EMBL-EBI (https://www.ebi.ac.uk/Tools/msa/clustalo/) with results viewed in MView. The red box highlights the position of K107 (SidA numbering). (c) Active site of SidA with bound L-Orn (PDB: 6x0j) overlayed with X-ray structures of DfoA (PDB: 5o8r) and NbtG (PDB: 4d7e) and a homology model of FbsI generated using SWISS model (https://swissmodel.expasy.org/). These NMOs are denoted with color-coded stars in the phylogenetic tree in panel (a).

review by the Tischler group²⁸ classified flavin-dependent NMOs, including siderophore-related NMOs. Phylogenetic analysis of characterized NMOs reveals grouping by substrate, but the sequence drivers for these groupings was not investigated. We performed a pairwise sequence analysis of 30 siderophore-related NMOs to better understand the high selectivity of FbsI for Putr. We selected a variety of NMOs representing substrate specificity for diamines, including Putr, cadaverine, Lys, and Orn (Figure 4a). FbsI clearly groups with NMOs acting on cadaverine and Putr diamine substrates. Pairwise analysis of the aligned set of 30 NMO protein sequences revealed that a conserved Lys residue (K107–SidA numbering) is present in all NMOs that N-hydroxylate Lys/Orn diamino acid substrates (Figure 4b). This Lys residue is replaced by either Ala or Ser in NMOs that act on cadaverine

and Putr diamine substrates. The only exception to this is BibB, which is presented in the literature as a cadaverine NMO, while our sequence analysis suggests BibB is more likely a Lys NMO. The liganded X-ray structure of SidA shows that K107 electrostatically interacts with the α -carboxylate group of the bound zwitterionic L-Orn (Figure 4c). Overlay of SidA, NbtG, DfoA, and a homology model of FbsI structures suggests that K107 could introduce an electrostatic repulsion with cationic diamine substrates. Thus, K107 and functionally equivalent positions in NMOs might serve as a predictive element for substrate specificity. Charge neutral amino acids like Ala and Ser at this position might better accommodate cationic diamine substrates like cadaverine/Putr, while the cationic Lys at this position might better stabilize zwitterionic substrates like Lys/Orn.

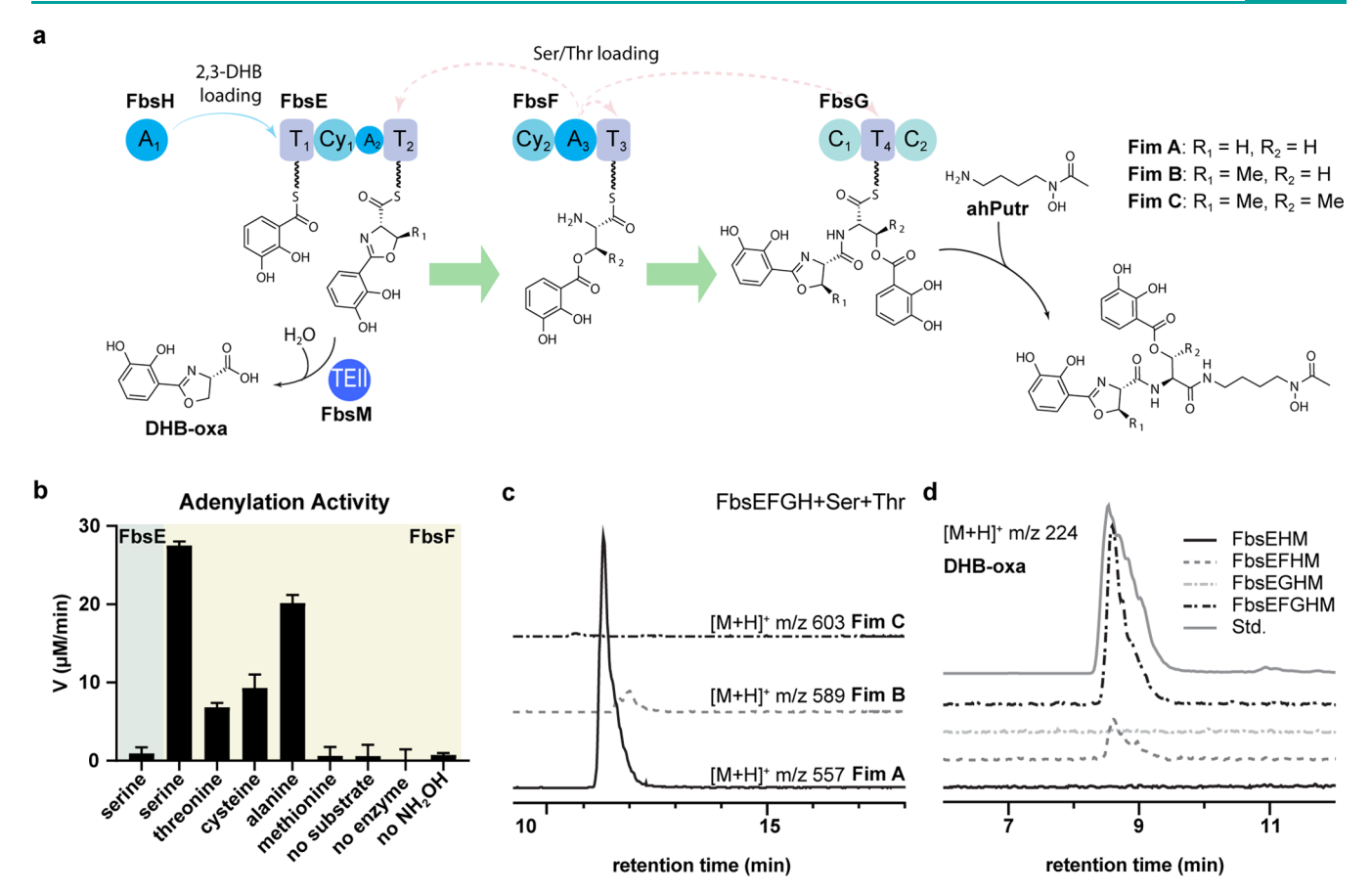


Figure 5. Chemoenzymatic synthesis of fimsbactin A via *in vitro* reconstitution of the FbsEFGH NRPS assembly line. (a) Overview of the fimsbactin NRPS assembly line with proposed thioester-tethered intermediates and arrows from A-domains to predicted substrate T-domains. (b) Apparent velocity (V) from AMP-formation assay using FbsE and FbsF and a variety of amino acid substrates. (c) EIC chromatograms for the expected [M + H]⁺ molecular ions corresponding to products fimsbactin A, B, and C from LC–MS analysis (2 h time point) of complete FbsEFGH reactions using a 1:1:1 mixture of DHB:Ser:Thr. (d) EIC chromatograms for the expected [M + H]⁺ molecular ion corresponding to DHB-oxa from LC–MS analysis (2 h time point) of FbsEFGHM reactions using a 1:1 mixture of DHB:Ser. All experiments were performed in duplicate as independent trials. LC–MS EIC traces were normalized to an internal Fmoc-Ala-OH standard. Error bars represent standard deviations.

Substrate Selectivity of Adenylation Domains in FbsEFH. The A-domains of NRPS modules catalyze the reversible adenylation of carboxylic acid substrates to generate the corresponding acyl adenylate intermediates with the release of PP_i to the solvent. In a second step, the A-domain catalyzes nucleophilic acyl substitution between the bound acyl adenylate and the PPant thiolate of the accommodated cognate T-domain to form the thioester-tethered substrateloaded T-domain with the release of AMP.³⁶ Thus, NRPS Adomains serve as a "gatekeeper" for the incorporation of precursor molecules into the assembled peptide scaffolds. There are four substrate loadings (2xDHB and 2xSer) required to assemble the fimsbactin A scaffold, yet only two complete Adomains are present in the NRPS modules (Figures 1, 2, 5a, and S2). FbsH shows the greatest homology to standalone DHB-activating A-domains, while FbsF contains an embedded A-domain predicted to activate Ser/Thr. This suggests that both FbsH and FbsF act twice to load the T-domains present in NRPS modules FbsEFG.

We used LC-MS analysis to directly detect the stable DHB acyl adenylate formed by FbsH (A $_1$ -domain), confirming its predicted role as an aryl-adenylating enzyme to activate the substrate DHB (Figure S7). The Ser/Thr acyl adenylates are not easily detected by LC-MS, so we used hydroxylamine to

intercept the acyl adenylate and release AMP, which was quantified using a coupled myokinase/pyruvate kinase/lactate dehydrogenase assay with continuous measurement of optical absorbance at 340 nm to determine the apparent rate of NADH oxidation as a proxy for AMP formation (Figure S8).³⁷ We used apo-FbsE and apo-FbsF lacking the PPant posttranslational modification on the T-domains to probe only the adenylating activity of the A-domains. As expected, FbsE, which contains a truncated A-domain void of the essential substrate and ATP-binding motifs, lacked the ability to adenylate L-Ser (Figure 5b). The truncated FbsE-A2-domain might serve a structural role needed to facilitate proteinprotein interactions within FbsE and between FbsE and other NRPS modules (FbsFGH). The FbsF A3-domain was able to adenylate L-Ser, L-Thr, L-Cys, and L-Ala but not the sterically larger amino acid L-Met supporting the observed incorporation of L-Ser and L-Thr into fimsbactin products. L-Ser produced the greatest apparent velocity, which is consistent with the apparent substrate preference leading to the formation of fimsbactin A (derived from 2xSer) as the major product isolated from A. baumannii and A. baylyi cultures. 8,14 Adenylation of L-Ala and L-Cys by FbsF was surprising, given these amino acids have not been observed in fimsbactin analogues from cell cultures. Adenylation of L-Ala and L-Cys is

consistent with similar steric size to L-Ser and L-Thr. Under dynamic equilibrium conditions, and given that adenylation is reversible, L-Ala is unlikely to carry forward through the NRPS loading and chain extension, given it lacks the β -hydroxyl group needed for cyclodehydration to the oxazoline intermediate. The lack of thiol or thiazoline-containing fimsbactin analogues suggests the C-domains and Cyc-domains in FbsEFG are selective for Ser/Thr over Cys in flux through the assembly line. These findings confirm that the FbsF A_3 -domain is the only adenylation domain that activates Ser/Thr to support fimsbactin biosynthesis.

Chemoenzymatic Synthesis of Fimsbactin A, B, and C via In Vitro Reconstitution of NRPS Modules FbsEFGH. We performed in vitro enzyme reactions using synthetic ahPutr in combination with DHB, L-Ser/L-Thr, ATP, and the complete NRPS assembly line consisting of FbsEFGH. The NRPS modules FbsEFG containing T-domains were primed for the in vitro reactions using phosphopantetheinyl transferase (PPTase) and coenzyme-A to install the required PPant prosthetic group. Reactions with DHB, ahPutr, and L-Ser produced a peak in the LC-MS EIC chromatogram that matched the authentic standard of fimsbactin A with retention time ~11.5 min and observed m/z = 574.9 (expected [M + H]⁺ m/z = 575.2) (Figure S9a). Reactions with DHB, ahPutr, and L-Thr produced a peak in the LC-MS EIC chromatogram that matched the authentic standard of fimsbactin C with retention time \sim 12.8 min and observed m/z = 603.0 (expected $[M + H]^+$ m/z = 603.2) (Figure S9a). Reactions with DHB, ahPutr, and a 1:1 mixtures of L-Ser:L-Thr produced a ~11:1 mixture of fimsbactin A:B and no detectable fimsbactin C (Figure 5c), which is consistent with the product ratios isolated from cultures of A. baumannii and A. baylyi. A screen of 23 benzoic acid substrates revealed high selectivity for the incorporation of 2,3-DHB into the final product (Figure S10). The formation of fimsbactin products under these cell-free conditions was dependent on time and the presence of all enzymes, FbsEFGH, ATP, and substrates (Figure S11). These results are consistent with the observed A-domain preference for L-Ser over L-Thr, indicating that the FbsF A₃-domain serves as a selectivity filter for the NRPS assembly line.

The use of synthetic ahPutr with the exclusion of FbsIJK is consistent with the mechanistic hypothesis where the terminal C₂-domain of FbsG reversibly binds to ahPutr and facilitates its nucleophilic attack on the FbsG-T₄-domain thioester-tethered substrate releasing fimsbactin A (Figure 5a). We also achieved the complete enzymatic synthesis of fimsbactin using a sevenenzyme combination consisting of FbsEFGHIJK, starting from L-Orn, acetyl-CoA, DHB, L-Ser, and all necessary cofactors (PLP, FAD) and cosubstrates (ATP, NADPH, O₂) (Figure S12). The use of FbsIJK to generate ahPutr in situ also generated aPutr as a side-product, which led to the formation of deoxy-fimsbactin A analogous to the presumed biosynthesis of fimsbactin D in A. baylyi arising from the incorporation of acetyl-diaminopropane (Figure 2). FbsIJK were capable of incorporating longer chain acyl groups, octanoyl, and decanoyl into the N_1 -acyl- N_1 -hydroxy-putrescine precursor, but these failed to be incorporated into the fimsbactin scaffold, reflecting selectivity for the final termination step presumably catalyzed by FbsG (Figure S12). This is consistent with similar acyl group promiscuity observed for DesABC in ferrioxamine biosynthesis.³⁸ It appears the standalone TEII domain, FbsM, is not required for functionality of the FbsEFGH machinery

under cell-free conditions, leading us to investigate the role of FbsM in fimsbactin biosynthesis.

FbsM is a Type II Thioesterase That Hydrolyzes the T-Domain-Tethered DHB-Oxa Thioesters. Thioesterase (TE) domains are α/β -hydrolases that commonly appear in NRPS assembly lines and catalyze a variety of reactions on Tdomain PPant-tethered peptidyl thioester substrates, including hydrolysis,³⁹ epimerization,⁴⁰ transacylation,¹⁹ lactamization,⁴ and lactonization. 42,43 Type I TE-domains (TEI) are frequently present in NRPS terminating modules, where they catalyze the hydrolytic release of peptides often via macrolactamization or macrolactonization to give cyclic peptide and depsipeptide products, respectively. 44,45 Type II TE-domains (TEII) are less common and occur as standalone domains that act in trans on T-domain thioester substrates. Standalone TEII domains have been shown to facilitate acyl transfer between Tdomains in NRPS modules, 19 but that does not seem to be an essential function for FbsM, given that the NRPS machinery FbsEFGH is capable of fimsbactin A production in the absence of FbsM. Under our in vitro conditions, the apparent rate of fimsbactin A formation via chemoenzymatic synthesis by FbsEFGH from DHB, L-Ser, and ahPutr was not obviously enhanced in the presence of FbsM, arguing against a kinetic role facilitating inter- and intrachain acyl transfers (Figure S7). The fbsM and fbsL genes are encoded for transcription in the opposite direction of other fimsbactin biosynthesis genes (Figure S1). These genes are apparently regulated by a different Fur box. Despite the opposite direction of transcription, the shared upstream Fur box suggests that fbsM and fbsL are coregulated with other fimsbactin biosynthesis genes, and expression of these genes might enhance fimsbactin production inside the cell.

TEII domains have also been shown to serve a proofreading function in the hydrolysis of mis-primed T-domains, where acyl-CoA derivatives are loaded by PPTase, leading to "capped" T-domains that incapacitate NRPS modules from shuttling the thioester-tethered substrates through the pathway and reducing metabolic flux. 46,47 While we did not directly test the ability of FbsM to recover the activity of mis-primed Tdomains, we did search for the presence of new metabolites arising from premature cleavage of thioester-tethered substrates. We observed a significant increase in the formation of DHB-oxa from the complete FbsEFGH reaction containing FbsM, which came with the complete consumption of the DHB acyl adenylate at the 3 h time point (Figure 5d). We confirmed the identity of DHB-oxa from the enzyme reactions using a synthetic standard of DHB-oxa (Scheme S2). As expected, reactions lacking FbsF, which contains the essential L-Ser activating A₃-domain, failed to generate DHB-oxa (Figure 5d). The presence of FbsG enhances levels of DHB-oxa by \sim 5fold, presumably via increased flux through the NRPS assembly line requiring FbsG as the termination module responsible for the release of the final product to achieve enzyme turnover. These results are consistent with FbsM-mediated hydrolysis of DHB-oxa from T-domains in the NRPS assembly line (Figure 5a). It is not clear if there is a preferred substrate or substrates for FbsM, given that the DHB-oxa thioester intermediate could conceivably form on the FbsE-T₂-domain, the FbsF-T₃domain, and/or the FbsG-T₄-domain (Figure 6b).

One additional role observed for hydrolases associated specifically with siderophore pathways is in the maturation or degradation of siderophores during export and/or import. The siderophore pyoverdine in *Pseudomonas aeruginosa* requires a

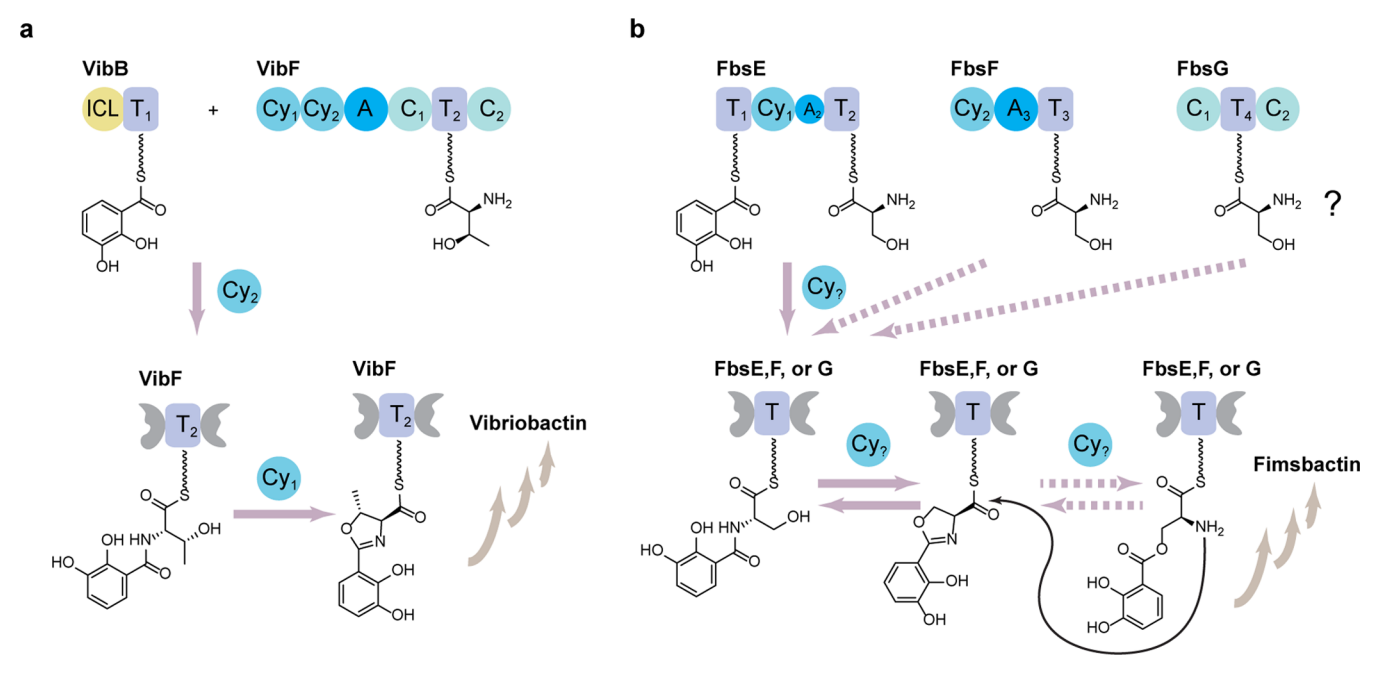


Figure 6. (a) Formation of DHB-methyloxazoline by VibB and VibF in vibriobactin biosynthetic pathway. (b) Mechanistic proposal for the *N*- and *O*-acylation of the central Ser unit of fimsbactin A via reversible equilibrium formation of T-domain PPant thioester-tethered *N*-DHB-Ser, *O*-DHB-Ser, and DHB-oxa by the Cy₁ and Cy₂ domains of FbsE and FbsF, respectively.

periplasmic deacetylase, PvdQ, to direct the peptide scaffold for final biosynthetic tailoring to install the fluorescent chromophore prior to efflux. The siderophore enterobactin in uropathogenic E. coli boasts one of the highest recorded apparent ferric stability constants on the order of 10⁴⁹.50 Harvesting the ferric complex requires hydrolysis of the triserine-lactone backbone by the periplasmic hydrolase IroD to form linearized enterobactin and DHB-Ser fragments with reduced affinity for ferric ion. 51 The isolation of fimsbactin F, which lacks the O-linked DHB moiety, inspired us to consider hydrolysis of fimsbactin A to fimsbactin F as a potential role for FbsM. However, fimsbactin A in metal-free and ferric complex forms proved to be stable in the presence of FbsM, with no detection of hydrolysis products as judged by LC-MS analysis of the reaction mixtures. We did not observe the formation of fimsbactin F during any of the enzyme-catalyzed reactions with combinations of FbsEFGHIJKM, leading us to believe this is a product only of fermentation, perhaps resulting from hydrolysis by a nonspecific esterase (Figure S9). Thus, we assign a shunting function to FbsM where DHB-oxa is cleaved from FbsE, FbsF, and/or FbsG to improve flux through the NRPS pathway and diversify the pool of metal chelators during fimsbactin biosynthesis. DHB-oxa and related NRPS shunt metabolites such DHB-Ser,⁵² vulnicibactin 2,⁵³ dihydroaeruginoic acid,⁵⁴ and escherechelin⁵⁵ have been shown to influence siderophore-mediated iron acquisition in producing pathogens and neighboring microbiomes. Our findings provide an enzymatic link to the production of DHB-oxa in A. baumannii through the biochemical characterization of the TEII FbsM. These findings will aid in the development of siderophore-related molecules as agonists and antagonists of siderophore pathways in target pathogens as an antivirulence strategy.5,6

Mechanistic Considerations. The branched chemical structure of fimsbactin A and the unusual domain architecture of the FbsEFG NRPS modules introduce a potentially new

biosynthetic paradigm for peptides with structures that branch through amide- and/or ester-bond linkages. The mechanism for N- and O-acylation of L-Ser in the fimsbactin NRPS assembly line is central to understanding this chemical logic. A related branching event takes place during vibriobactin biosynthesis where the three nitrogens of norspermidine are sequentially acylated with one unit of DHB and two units of DHB-methyloxazoline. The first N_1 -acylation is facilitated between norspermidine and the VibB T-domain DHB-PPant thioester (derived via activation by DHB-selective VibE Adomain) by the standalone C-domain VibH to produce amidelinked N_1 -DHB-norspermidine.²⁰ The largest NRPS module, VibF, contains a Cy₁-Cy₂-A-C₁-T-C₂ domain orientation. The VibF A-domain activates and loads L-Thr as the corresponding thioester to the internal T-domain. Next, Cy2 facilitates amide bond formation between the Thr-loaded VibF T-domain and the DHB-loaded VibB T-domain to give DHB-Thr tethered as the corresponding PPant thioester to the VibE T-domain. Cy1 then catalyzes the cyclodehydration of the tethered DHB-Thr to DHB-methyloxazoline thioester (Figure 6a).56 This intermediate is later captured in two separate acylation reactions with the N_5 - and N_9 -amino groups of N_1 -DHBnorspermidine both catalyzed by the C2-domain of VibF to give the mature amide-branched vibriobactin structure.⁵⁷ The VibF-C₁-domain was found to be catalytically inactive but seems to serve as a dimerization element to promote interchain adenylation, acyl transfer, and cyclodehydration reactions during peptide assembly.⁵⁸ The same roles for FbsE-Cy₁ (VibF-Cy₁), FbsF-Cy₂ (VibF-Cy₂), FbsG-C₁ (VibF-C₁), and FbsG-C₂ (VibF-C₂) could be assigned for the fimsbactin NRPS assembly line based on sequence homology (Figure S13), but there is a noticeable difference in the number of T-domains that suggests a slightly different mechanism is at play.

The number of T-domains present in the vibriobactin (2) and fimsbactin (4) NRPS assembly lines is different while the number (2) and selectivity (DHB and Ser/Thr) of catalytically

active A-domains is functionally retained. The presence of additional T-domains suggests that the accumulation of additional T-domain thioester-tethered intermediates is required for fimsbactin biosynthesis beyond the DHB, Ser/ Thr, and DHB-oxa thioesters that are required to produce vibriobactin.20 This suggestion is consistent with the occurrence of DHB-oxa and O-DHB-Ser in the mature fimsbactin A scaffold. We propose that the oxazoline (DHBoxa) thioester serves as a central intermediate equilibrating between the amide (N-DHB-Ser) and ester (O-DHB-Ser) forms with distribution across FbsE (T2), FbsF (T3), and FbsG (T_3) , meeting the demands of flux through the NRPS assembly line (Figure 6b). This proposal is consistent with the known reversibility of NRPS C-domains⁵⁹ and the known chemistry of oxazolines.⁶⁰ The hydrolysis of oxazolines is pH-dependent, where the amide product is favored at higher pH and the ester product is favored at lower pH. The kinetics of hydrolysis for DHB-oxa thioesters could be controlled in the Cy- or Cdomain active sites. The phenolate-methyl-oxazoline moiety in the structurally related siderophore serratiochelin (Figure 1) was reported to undergo a nonenzymatic hydrolysis under acidic conditions (2% formic acid) to produce an O-acylated DHB ester with L-Thr. 21 A reversible distribution of T-domain thioester intermediates is consistent with the formation of known biosynthetic shunt products (fimsbactin E, fimsbactin F, and DHB-oxa) and requires a selection element to balance metabolic flux.

We propose that the standalone TEII domain FbsM serves as a "traffic control" element through the selective cleavage of DHB-oxa thioester intermediates from FbsE, FbsF, and FbsG. While the preferred site of DHB-oxa hydrolysis is not yet known (FbsE, FbsF, or FbsG), we did observe an increase in the rate of DHB-oxa formation with the addition of FbsG (Figure 5d). This is consistent with the upstream formation of DHB-oxa on FbsE and/or FbsF, with more DHB-oxa forming in the presence of FbsG due in part to increased flux and/or the unwanted accumulation of DHB-oxa-thioester tethered to the FbsG-T₄-domain. The direct hydrolysis of an FbsG DHBoxa thioester could be necessary to bias the accumulation of an O-DHB-Ser thioester intermediate at this site, which provides the free amino group necessary to accept an interchain acyl transfer from a DHB-oxa thioester tethered to an upstream Tdomain (Figures 5a and 6b). The functional diversity across the TE enzyme family makes functional prediction difficult based on sequence and structural comparison (Figure S14).⁶¹ Here, we clearly demonstrated that FbsM is not essential for fimsbactin A biosynthesis in our cell-free enzyme-mediated system (Figure 5c). This result suggests that FbsM does not facilitate any essential intra- and interchain acyl transfers, although a kinetic effect of this sort cannot be ruled out without direct testing. The TEII LgnA was recently shown to facilitate interchain acyl transfer of Thr between the T-domains of NRPS modules LgnB and LgnD during legonindolizidine A biosynthesis.¹⁹ However, the thermodynamics of this acyl transfer remain paradoxical, given that LgnA contains an active site Ser residue that provides an intermediate LgnA-Ser-oxo ester, which is thermodynamically more stable than the LgnB and LgnD thioesters. Additional factors that might be present in the cell such as misloaded T-domains and constraints on metabolic flux might make FbsM conditionally essential for fimasbactin A biosynthesis during fermentation.

Following the lines of mechanistic thought discussed thus far, an inclusive mechanism for the NRPS assembly line

ı

portion of fimsbactin A biosynthesis can be proposed (Figure 6b). FbsH adenylates DHB and loads the T₁-domain of FbsE to afford the corresponding FbsE-T₁-DHB thioester. The A₃domain of FbsF adenylates Ser and loads the T2-domain of FbsE (interchain) and the T₃-domain of FbsF (intrachain) as the corresponding Ser thioesters. The embedded Cy₁-domain of FbsE presumably facilitates amide bond formation between the FbsE-T₁-DHB/FbsE-T₂-Ser thioesters and the FbsE-T₁-DHB/FbsF-T₃-Ser thioesters to produce the FbsE-T₂- and FbsF-T3-tethered N-DHB-Ser thioesters. Subsequent cyclodehydration catalyzed by FbsF-Cy2 could produce the FbsE-T₂-DHB-oxa (interchain) and FbsF-T₃-DHB-oxa (intrachain) thioesters. Further, either FbsE-Cy₁ or FbsF-Cy₂ could hydrolyze the FbsE-T₂-DHB-oxa and FbsF-T₃-DHB-oxa thioesters to the corresponding O-DHB-Ser thioesters. Collectively, it is conceivable to form a mixed pool of N-DHB-Ser, O-DHB-Ser, and DHB-oxa that can be transferred directly to FbsG-T₄ via interchain acyl group transfer catalyzed by FbsG-C₂. We also cannot rule out the possibility of direct loading of FbsG-T₄ with Ser by FbsE-A₃ followed by the analogous formation of FbsG-T₄ thioesters with N-DHB-Ser, O-DHB-Ser, and DHB-oxa. At some point, it seems likely for an FbsG-T₄-O-DHB-Ser thioester to form, where FbsG-C₁ facilitates acyl transfer with a DHB-oxa thioester to form the FbsG-T₄-(O-DHB-Ser)-N-DHB-oxa intermediate. Intermolecular cleavage of this thioester by ahPutr, presumably catalyzed by FbsG-C2, would provide the complete fimsbactin A structure and achieve enzymatic turnover.

SUMMARY AND CONCLUSIONS

A cell-free chemoenzymatic synthesis of the siderophore fimsbactin A, a small molecule iron scavenging virulence factor produced by human pathogenic A. baumannii, was achieved via in vitro reconstitution of recombinant enzymes FbsEFGHIJKM that were purified from heterologous expression in E. coli. The conversion of L-Orn to ahPutr was facilitated by the ordered action of PLP-dependent decarboxylase FbsJ, flavin-dependent NMO FbsI, and N-acetyltransferase FbsK. The substrate selectivity of NMO FbsI for catalyzing mono-N-hydroxylation of putrescine was established, and sequence analysis of the NMO family revealed an active site signature associated with diamine or diamino acid substrate preference. The conversion of ahPutr, DHB, and L-Ser to fimsbactin A was completed using the NRPS machinery FbsH (DHB-selective A₁-domain), FbsE (NRPS elongation module with T_1 - Cy_1 - A_2 - T_2 domains; A2 is catalytically inactive), FbsF (NRPS elongation module with Cy₂-A₃-T₃; A₃ is selective for Ser), and FbsG (NRPS termination module with C₁-T₄-C₂ domains). The NRPSassociated TEII domain FbsM selectively hydrolyzes DHB-oxa, a metal chelating shunt metabolite, from thioester-tethered Tdomain intermediates. A mechanism is proposed where the FbsE-Cy₁ and FbsF-Cy₂ domains partition T-domain-tethered DHB-oxa intermediates, between N-DHB-Ser and O-DHB-Ser thioester intermediates accounting for the branching Ser residue with amide and ester linkages. The terminating NRPS modules FbsG contains a C-T-C motif that facilitates nucleophilic attack of ahPutr on a O-DHB-Ser-N-DHB-oxa thioester intermediate to release fimsbactin A as the final product. The terminating C-T-C motif could be a common element for producing branched peptide scaffolds from NRPS assembly lines.

EXPERIMENTAL SECTION

Materials, Methods, and Instrumentation. All enzymes, cofactors, buffers, and reagents were purchased from Sigma-Aldrich (St. Louis, MO) unless otherwise stated. E. coli BL21-Gold (DE3) and E. coli TOP10 were purchased from Agilent and Invitrogen, respectively. E. coli cells were made chemically competent by standard methods. The strain of A. baumannii ATCC 17978 was purchased from the American Type Culture Collection (ATCC). Bacteria were stored as frozen glycerol stocks at $-80\,^{\circ}\text{C}$. Genomic DNA of A. baumannii ATCC 17978 was purified with DNeasy Blood and Tissue Kit from Qiagen, following standard protocols. Primers were purchased from Integrated DNA Technologies, Inc., for DNA amplification. Coding sequences were prepared via polymerase chain reaction (PCR) amplification with Phusion polymerase from Thermo Fisher. Samples for LC-MS were prepared in 0.45 μ poly(tetrafluoroethylene) (PTFE) Mini-UniPrep vials from Agilent. LC-MS analyses were performed using an Agilent 6130 quadrupole with G1367B autosampler, G1315 diode array detector, 1200 series solvent module. A Phenomenex Gemini C18 column (50 × 2 mm), 5 μm with guard column was used for all LC-MS analyses. LC-MS mobile phases were 0.1% formic acid in (A) H₂O and (B) acetonitrile, and LC-MS data were processed using G2710 ChemStation software (Agilent). Preparative HPLC was performed on an Agilent/HP 1050 quaternary pump module with an Agilent/HP 1050 MWD module using a Phenomenex Luna 10μ C18(2) 100A column, 250 × 21.2 mm, 10 μ m with guard column. NMR was performed on a Varian Unity Plus-300 MHz instrument. The maximum likelihood phylogenetic trees of selected NMOs and thioesterases were built by the PhyML+SMS/OneClick method with 100 boost trap replicates from NGPhylogeny.fr⁶² and visualized using iTOL v6.⁶³ Sequence alignments were performed by the Clustal Omega online tool from EMBL.⁶⁴ The alignment results were viewed in ESPript 3.0.⁶

Cloning, Expression, and Protein Purification. Forward and reverse primers (Table S5) were designed to amplify specific region of genes (fbsE-K, fbsM) and insert restriction enzyme cutting sites using A. baumannii ATCC 17978 genomic DNA as a template. The gene amplification was done by polymerase chain reaction (PCR) with Phusion polymerase, and the resulting PCR products were analyzed by DNA gel electrophoresis and purified with Monarch PCR & DNA cleanup kit. Purified PCR fragments and pET28a vector were separately digested with either FD-NdeI and FD-HindII or FD-BamHI and FD-NdeI. The cut vector was purified with Monarch PCR & DNA cleanup kit and used directly in an overnight ligation reaction with the targeted gene and T4 DNA ligase at 16 °C. The ligated plasmids harboring the targeted genes were used to transform the chemically competent E. coli TOP10 cells, which were plated on an antibiotic selection agar plate containing 50 µg/mL kanamycin to select cells with the correct clones. Sanger sequencing was performed by Genewiz to confirm the desired constructs (Tables S3 and S4). The confirmed plasmids were used to transform the chemically competent E. coli BL21(DE3) cells for expression purpose.

For protein expression, E. coli BL21 cells harboring the appropriate genes were grown overnight at 37 °C in a 5 mL LB containing 50 μ g/ mL kanamycin with gentle agitation. A 1 mL aliquot of the overnight cell culture was used to inoculate 1 L terrific broth (12 g/L tryptone, 24 g/L yeast extract, 5 g/L glycerol, 17 mM KH₂PO₄, and 72 mM K_2PO_4) containing 50 μ g/mL kanamycin. The cell culture was grown at 37 $^{\circ}$ C with agitation until OD₆₀₀ reached 0.4–0.8. The culture was cooled on an ice bath for 20 min before being treated with 1 mL of 0.5 M IPTG to induce protein overexpression. The induced cultures were incubated at 18 °C with agitation for 18 h. All subsequent protein purification steps were performed at 4 $^{\circ}\text{C}$. After spinning the cell culture at 5000 rpm for 30 min, the supernatant was discarded and the pelleted cells were resuspended in a 40 mL resuspension buffer (50 mM K₂HPO₄, 500 mM NaCl, 5 mM BME, 20 mM imidazole, 10% glycerol, SIGMAFST protease inhibitor, pH 8). Cell suspension was flash-frozen in liquid nitrogen, thawed, and lysed by passing through an EmulsiFlex C5 cell disruptor (Avestin). The lysed cell was pelleted by ultracentrifugation (45,000 rpm, 30 min), and the

resulting supernatant was loaded on a column of Ni-NTA resin preequilibrated with wash buffer (50 mM K2HPO4, 500 mM NaCl, 5 mM BME, 20 mM imidazole, 10% glycerol, pH 8). After 30 min of incubation, the column flow-through was discarded, and the resin was washed with wash buffer (2 × 40 mL) prior to the elution of His6tagged protein with 4 × 15 mL portions of elution buffer (50 mM K₂HPO₄, 500 mM NaCl, 5 mM BME, 300 mM imidazole, 10% glycerol, pH 8). Elution fractions were combined and dialyzed in 1 L phosphate buffer (50 mM K₂HPO₄, 500 mM NaCl, 1 mM DTT, pH 8) for ~18 h using 10,000 MWCO SnakeSkin dialysis tubing. The purified protein solution was concentrated by centrifugal filtration using Amicon Ultra centrifugal unit (15 mL, 30 or 100 kDa MWCO, depending on the molecular weight of the targeted protein) and flashfrozen in liquid nitrogen as $\sim 50 \mu L$ aliquots. The purities of proteins were judged by sodium dodecyl sulfate-polyacrylamide gel electrophoresis (SDS-PAGE) with any kD SDS-PAGE gels purchased from Bio-Rad. All frozen proteins were stored at -80 °C.

NAD(P)H Oxidation Assay. As the hydroxylation of substrates by FbsI requires reducing agents, we adopted an NAD(P)H oxidation assay to determine the substrate preference of FbsI. The assay was performed on a 96-well plate with a volume size of 200 μ L. The reaction solution consisted of 100 mM MOPS (pH 7.0), 50 µM FAD, 50 μ M PLP, 2 mM putrescine, 1 μ M FbsI, and 1 μ M FbsI (when needed). Reactants were carefully mixed and incubated for 5 min before adding the NAD(P)H cofactor to initiate. Considering that NAD(P)H oxidation can be promoted by free FAD, the blank consisted of a solution with FAD, NAD(P)H, no substrate, and no enzyme. Furthermore, the NAD(P)H oxidation in the presence of both FAD and FbsI was measured to evaluate if the enzyme can further promote NAD(P)H oxidation in the absence of substrate, and the resulting measured activity was compared with the activity measured in the presence of substrates. Each condition was tested in duplicate. Data were collected by SpectraMax Plus 384 microplate reader (Molecular Devices). Absorbance at 340 nm was monitored for 30 min at 37 $^{\circ}$ C using an interval of 10 seconds.

Reconstitution of ahPutr Biosynthesis. For the optimized ahPutr production, we employed an NADPH regeneration system to ensure a steady supply of reducing equivalents. Reaction mixtures for ahPutr production were prepared in 100 mM TAPS buffer (pH 8) with final working concentrations of 2 mM ornithine, 0.05 mM PLP, 0.05 mM FAD, 2.5 mM acetyl-CoA, 10% glycerol, 2.5 mM ATP, 15 mM MgCl₂, 10 μ M FbsI, 10 μ M FbsJ, 10 μ M FbsK, and the NADPH regeneration system (40 mM glucose-6-phosphate, 4 mM NADP+, 1 mM MgCl₂, and 4 U/mL glucose-6-phosphate dehydrogenase).⁶⁶ The regeneration system was incubated at 37 °C for 1 h to generate NADPH before being used in the reactions, and FbsJ was added last to initiate the reaction. At each time point, 100 μ L aliquots of the reaction mixtures were taken out and incubated with 260 µL acetonitrile, 100 μ L of 0.2 M sodium borate, 40 μ L of 20 mM Fmoc-Cl, and 100 μ L of 1.2 mM Fmoc-Ala-OH for 30 min at room temperature. The samples were centrifuged, filtered, and analyzed via LC-MS.

Delineation of ahPutr Biosynthesis Reaction Order. To simplify the reaction, putrescine was used as the direct substrate in this assay. The reaction mixtures were prepared in 100 mM TAPS buffer (pH 8) with the aforementioned NADPH regeneration system, and it consisted of final concentrations of 5 mM putrescine, 0.05 mM FAD, 5 mM acetyl-CoA, 3 mM ATP, 10% glycerol, and 15 mM MgCl₂. To delineate the reaction order, two sets of reactions were prepared: (1) the reaction was first incubated with 25 μ M FbsI for 2 h and then added with 25 μ M FbsK and reacted for another 2 h; (2) the reaction was incubated with 25 μ M FbsK for 2 h and then added with $25 \mu M$ FbsI and reacted for another 2 h. At 2 and 4 h time points, 100 μ L aliquots of the reaction mixture were taken out and incubated with 260 μ L acetonitrile, 100 μ L of 0.2 M sodium borate, 40 μ L of 20 mM Fmoc-Cl, and 100 μ L of 1.2 mM Fmoc-Ala-OH for 30 min at room temperature. The samples were centrifuged, filtered, and analyzed via LC-MS.

Synthesis of ahPutr and DHB-Oxa. See the Supporting Information document for synthetic details, compound character-

ization data, and purity analysis (Figures S15–S28 and Schemes S1–S2).

Hydroxylamine-Promoted AMP Release Assay. The assay was performed on a 96-well plate with a volume size of 200 μ L. The reaction mixtures consisted of 50 mM Tris (pH 8), 0.2 mM NADH, 5 mM ATP, 4 U/mL myokinase, 8.4 U/mL pyruvate kinase, 12.6 U/mL lactate dehydrogenase, 1 mM PEP, 5 mM MgCl₂, 32 mM hydroxylamine (pH 7.2), 2 μ M apo-FbsF or apo-FbsE, and 2 mM selected amino acids (serine, threonine, cysteine, alanine, or methionine). Controls were prepared in the absence of substrate, enzyme, or hydroxylamine. The reactions were initiated with the addition of NPRS enzymes and performed in duplicate. Data were collected by SpectraMax Plus 384 microplate reader (Molecular Devices). Absorbance at 340 nm was monitored for 5 min at room temperature using an interval of 12 seconds.

In Vitro Reconstitution of Fimsbactin Biosynthesis. The pantetheinylated NRPS modules were prepared by incubating 25 μ M apo-FbsE, apo-FbsF, or apo-FbsG in 75 mM in Tris buffer (pH 8) with 180 μ M CoASH, 5 mM DTT, 10 mM MgCl₂, and 1 μ M Sfp at room temp for 2 h. To produce fimsbactin, 1 μ M FbsH, 1 μ M holo-FbsE, 1 μ M holo-FbsF, and 1 μ M holo-FbsG were mixed with 5 mM ATP, 10 mM MgCl₂, 5 mM DTT, 1 mM DHB, 1 mM ι -Ser and/or ι -Thr, and 0.5 mM ahPutr. The reactions were allowed to proceed for 3 h at 37 °C. Then, 100 μ L aliquots were quenched with 100 μ L MeOH. Samples were centrifuged, filtered, and subjected to LC-MS analysis. In the substrate preference study, DHB and ahPutr were substituted with other benzoic acids and cleaving nucleophiles, respectively.

FbsM Activity Assay. The pantetheinylated NRPS modules were prepared afresh, as described in the previous section. To test the activity of FbsM, 5 μ M FbsM was added to the complete fimsbactin reconstitution assay mixture containing FbsH, holo-FbsE, holo-FbsF, holo-FbsG, and all necessary substrates and reagents, as described in the previous section. The reaction was allowed to proceed for 24 h. At 3 and 24 h time points, 100 μ L aliquots of the reaction mixture were quenched with 100 μ L MeOH. Samples were centrifuged, filtered, and subjected to LC-MS analysis. A series of assays were performed similarly but in the absence of holo-FbsE, holo-FbsF, holo-FbsG, and/or FbsH.

ASSOCIATED CONTENT

Supporting Information

The Supporting Information is available free of charge at https://pubs.acs.org/doi/10.1021/acschembio.2c00573.

Supporting figures, tables, compound characterization data, and compound purity analyses (PDF)

AUTHOR INFORMATION

Corresponding Author

Timothy A. Wencewicz — Department of Chemistry, Washington University in St. Louis, St. Louis, Missouri 63130, United States; orcid.org/0000-0002-5839-6672; Phone: 314-935-7247; Email: wencewicz@wustl.edu; Fax: 314-935-4481

Author

Jinping Yang — Department of Chemistry, Washington University in St. Louis, St. Louis, Missouri 63130, United States

Complete contact information is available at: https://pubs.acs.org/10.1021/acschembio.2c00573

Notes

The authors declare no competing financial interest.

ACKNOWLEDGMENTS

The authors thank J. Kao and M. Singh for assistance with acquisition of NMR spectra in the Department of Chemistry at Washington University in St. Louis. The authors thank A. M. Gulick (University at Buffalo) for helpful discussions and collaborative studies related to the fimsbactin biosynthetic pathway. This research was supported by the National Science Foundation through NSF CAREER-1654611 award to T.A.W. Scholarship support was provided to J.Y. by the Dr. Max Wolfsberg Fellowship at Washington University in St. Louis.

ABBREVIATIONS

A, adenylation; ahPutr, N_1 -acetyl- N_1 -hydroxy-putrescine; ATCC, American Type Culture Collection; BGC, biosynthetic gene cluster; BME, 2-mercaptoethanol; C, condensation; Cy, cyclization; DHB, 2,3-dihydroxybenzoic acid; DHB-oxa, 2-(2,3-dihydroxyphenyl)-4,5-dihydrooxazole-4-carboxylic acid; DTT, dithiothreitol; hPutr, N-hydroxy-putrescine; N-DHB-Ser, N-(2,3-dihydroxybenzoyl)serine; O-DHB-Ser, O-(2,3-dihydroxybenzoyl)serine; Fim, fimsbactin; FMO, flavin monooxygenase; MDR, multi-drug resistant; NMO, N-hydroxylating monooxygenase; NRPS, nonribosomal peptide synthetase; NTA, nitrilotriacetic acid; PPant, phosphopantetheinyl; PPTase, phosphopantetheinyl transferase; Putr, putrescine; T, thiolation; TE, thioesterase

REFERENCES

- (1) Hider, R. C.; Kong, X. Chemistry and Biology of Siderophores. *Nat. Prod. Rep.* **2010**, *27*, 637–657.
- (2) Miethke, M.; Marahiel, M. A. Siderophore-Based Iron Acquisition and Pathogen Control. *Microbiol. Mol. Biol. Rev.* **2007**, 71, 413–451.
- (3) Miller, M. J.; Zhu, H.; Xu, Y.; Wu, C.; Walz, A. J.; Vergne, A.; Roosenberg, J. M.; Moraski, G.; Minnick, A. A.; McKee-Dolence, J.; et al. Utilization of Microbial Iron Assimilation Processes for the Development of New Antibiotics and Inspiration for the Design of New Anticancer Agents. *Biometals* 2009, 22, 61–75.
- (4) Yang, J.; Banas, V. S.; Patel, K. D.; Rivera, G. S. M.; Mydy, L. S.; Gulick, A. M.; Wencewicz, T. A. An Acyl-Adenylate Mimic Reveals the Structural Basis for Substrate Recognition by the Iterative Siderophore Synthetase DesD. J. Biol. Chem. 2022, 298, No. 102166.
- (5) Bohac, T. J.; Shapiro, J. A.; Wencewicz, T. A. Rigid Oxazole Acinetobactin Analog Blocks Siderophore Cycling in *Acinetobacter baumannii*. ACS Infect. Dis. **2017**, *3*, 802–806.
- (6) Bohac, T. J.; Fang, L.; Banas, V. S.; Giblin, D. E.; Wencewicz, T. A. Synthetic Mimics of Native Siderophores Disrupt Iron Trafficking in *Acinetobacter baumannii*. ACS Infect. Dis. **2021**, 7, 2138–2151.
- (7) Yamamoto, S.; Okujo, N.; Sakakibara, Y. Isolation and Structure Elucidation of Acinetobactin, a Novel Siderophore from Acinetobacter baumannii. *Arch. Microbiol.* **1994**, *162*, 249–254.
- (8) Proschak, A.; Lubuta, P.; Grün, P.; Löhr, F.; Wilharm, G.; De Berardinis, V.; Bode, H. B. Structure and Biosynthesis of Fimsbactins A-F, Siderophores from *Acinetobacter baumannii* and *Acinetobacter baylyi*. ChemBioChem **2013**, 14, 633–638.
- (9) Penwell, W. F.; DeGrace, N.; Tentarelli, S.; Gauthier, L.; Gilbert, C. M.; Arivett, B. A.; Miller, A. A.; Durand-Reville, T. F.; Joubran, C.; Actis, L. A. Discovery and Characterization of New Hydroxamate Siderophores, Baumannoferrin A and B, Produced by Acinetobacter baumannii. *ChemBioChem* **2015**, *16*, 1896–1904.
- (10) Shapiro, J. A.; Wencewicz, T. A. Acinetobactin Isomerization Enables Adaptive Iron Acquisition in *Acinetobacter baumannii* through PH-Triggered Siderophore Swapping. *ACS Infect. Dis.* **2016**, *2*, 157–168
- (11) Kim, M.; Kim, D. Y.; Song, W. Y.; Park, S. E.; Harrison, S. A.; Chazin, W. J.; Oh, M. H.; Kim, H. J. Distinctive Roles of Two

- Acinetobactin Isomers in Challenging Host Nutritional Immunity. *mBio* **2021**, *12*, No. e02248-21.
- (12) Sheldon, J. R.; Skaar, E. P. Acinetobacter baumannii Can Use Multiple Siderophores for Iron Acquisition, but Only Acinetobactin Is Required for Virulence. *PLoS Pathog.* **2020**, *16*, No. e1008995.
- (13) Bailey, D. C.; Bohac, T. J.; Shapiro, J. A.; Giblin, D. E.; Wencewicz, T. A.; Gulick, A. M. Crystal Structure of the Siderophore Binding Protein BauB Bound to an Unusual 2:1 Complex between Acinetobactin and Ferric Iron. *Biochemistry* **2018**, *57*, 6653–6661.
- (14) Bohac, T. J.; Fang, L.; Giblin, D. E.; Wencewicz, T. A. Fimsbactin and Acinetobactin Compete for the Periplasmic Siderophore Binding Protein BauB in Pathogenic *Acinetobacter baumannii*. *ACS Chem. Biol.* **2019**, *14*, 674–687.
- (15) Proschak, A.; Lubuta, P.; Gruen, P.; Loehr, F.; Wilharm, G.; De Berardinis, V.; Bode, H. B. Structure and Biosynthesis of Fimsbactins A-F, Siderophores from *Acinetobacter baumannii* and *Acinetobacter baylyi*. ChemBioChem **2013**, *14*, 633–638.
- (16) Beld, J.; Sonnenschein, E. C.; Vickery, C. R.; Noel, J. P.; Burkart, M. D. The Phosphopantetheinyl Transferases: Catalysis of a Post-Translational Modification Crucial for Life. *Nat. Prod. Rep.* **2014**, *31*, *61*–108.
- (17) Heathcote, M. L.; Staunton, J.; Leadlay, P. F. Role of Type II Thioesterases: Evidence for Removal of Short Acyl Chains Produced by Aberrant Decarboxylation of Chain Extender Units. *Chem. Biol.* **2001**, *8*, 207–220.
- (18) Fujimori, D. G.; Hrvatin, S.; Neumann, C. S.; Strieker, M.; Marahiel, M. A.; Walsh, C. T. Cloning and Characterization of the Biosynthetic Gene Cluster for Kutznerides. *Proc. Natl. Acad. Sci. U.S.A.* **2007**, *104*, 16498–16503.
- (19) Wang, S.; Brittain, W. D. G.; Zhang, Q.; Lu, Z.; Tong, M. H.; Wu, K.; Kyeremeh, K.; Jenner, M.; Yu, Y.; Cobb, S. L.; Deng, H. Aminoacyl Chain Translocation Catalysed by a Type II Thioesterase Domain in an Unusual Non-Ribosomal Peptide Synthetase. *Nat. Commun.* 2022, 13, No. 62.
- (20) Keating, T. A.; Marshall, C. G.; Walsh, C. T. Reconstitution and Characterization of the Vibrio Cholerae Vibriobactin Synthetase from VibB, VibE, VibF, and VibH. *Biochemistry* **2000**, *39*, 15522–15530.
- (21) Seyedsayamdost, M. R.; Cleto, S.; Carr, G.; Vlamakis, H.; João Vieira, M.; Kolter, R.; Clardy, J. Mixing and Matching Siderophore Clusters: Structure and Biosynthesis of Serratiochelins from Serratia Sp. V4. J. Am. Chem. Soc. 2012, 134, 13550–13553.
- (22) Song, W. Y.; Kim, H. J. Current Biochemical Understanding Regarding the Metabolism of Acinetobactin, the Major Siderophore of the Human Pathogen: *Acinetobacter baumannii*, and Outlook for Discovery of Novel Anti-Infectious Agents Based Thereon. *Nat. Prod. Rep.* **2020**, 477–487.
- (23) Naka, H.; Liu, M.; Actis, L. A.; Crosa, J. H. Plasmid- and Chromosome-Encoded Siderophore Anguibactin Systems Found in Marine Vibrios: Biosynthesis, Transport and Evolution. *Biometals* **2013**, *26*, 537–547.
- (24) Sattely, E. S.; Walsh, C. T. A Latent Oxazoline Electrophile for N-O-C Bond Formation in Pseudomonine Biosynthesis. *J. Am. Chem. Soc.* **2008**, *130*, 12282–12284.
- (25) May, J. J.; Kessler, N.; Marahiel, M. A.; Stubbs, M. T. Crystal Structure of DhbE, an Archetype for Aryl Acid Activating Domains of Modular Nonribosomal Peptide Synthetases. *Proc. Natl. Acad. Sci. U.S.A.* **2002**, *99*, 12120–12125.
- (26) Eisendle, M.; Oberegger, H.; Zadra, I.; Haas, H. The Siderophore System Is Essential for Viability of Aspergillus Nidulans: Functional Analysis of Two Genes Encoding l-Ornithine N 5-Monooxygenase (SidA) and a Non-Ribosomal Peptide Synthetase (SidC). *Mol. Microbiol.* **2003**, *49*, 359–375.
- (27) Li, B.; Lowe-Power, T.; Kurihara, S.; Gonzales, S.; Naidoo, J.; Macmillan, J. B.; Allen, C.; Michael, A. J. Functional Identification of Putrescine C- and N-Hydroxylases. *ACS Chem. Biol.* **2016**, *11*, 2782–2789.
- (28) Mügge, C.; Heine, T.; Baraibar, A. G.; van Berkel, W. J. H.; Paul, C. E.; Tischler, D. Flavin-Dependent N-Hydroxylating Enzymes:

- Distribution and Application. Appl. Microbiol. Biotechnol. 2020, 104, 6481-6499.
- (29) Franke, J.; Ishida, K.; Ishida-Ito, M.; Hertweck, C. Nitro versus Hydroxamate in Siderophores of Pathogenic Bacteria: Effect of Missing Hydroxylamine Protection in Malleobactin Biosynthesis. *Angew. Chem., Int. Ed.* **2013**, *52*, 8271–8275.
- (30) Salomone-Stagni, M.; Bartho, J. D.; Polsinelli, I.; Bellini, D.; Walsh, M. A.; Demitri, N.; Benini, S. A Complete Structural Characterization of the Desferrioxamine E Biosynthetic Pathway from the Fire Blight Pathogen Erwinia Amylovora. *J. Struct. Biol.* **2018**, 202, 236–249.
- (31) Heemstra, J. R.; Walsh, C. T.; Sattely, E. S. Enzymatic Tailoring of Ornithine in the Biosynthesis of the Rhizobium Cyclic Trihydroxamate Siderophore Vicibactin. *J. Am. Chem. Soc.* **2009**, 131, 15317–15329.
- (32) Kadi, N.; Song, L.; Challis, G. L. Bisucaberin Biosynthesis: An Adenylating Domain of the BibC Multi-Enzyme Catalyzes Cyclodimerization of N-Hydroxy-N-Succinylcadaverine. *Chem. Commun.* **2008**, 5119–5121.
- (33) Campbell, A. C.; Stiers, K. M.; Martin Del Campo, J. S.; Mehra-Chaudhary, R.; Sobrado, P.; Tanner, J. J. Trapping Conformational States of a Flavin-Dependent N-Monooxygenase in Crystallo Reveals Protein and Flavin Dynamics. *J. Biol. Chem.* **2020**, *295*, 13239–13250.
- (34) Binda, C.; Robinson, R. M.; Martin Del Campo, J. S.; Keul, N. D.; Rodriguez, P. J.; Robinson, H. H.; Mattevi, A.; Sobrado, P. An Unprecedented NADPH Domain Conformation in Lysine Monooxygenase NbtG Provides Insights into Uncoupling of Oxygen Consumption from Substrate Hydroxylation. *J. Biol. Chem.* **2015**, 290, 12676–12688.
- (35) Waterhouse, A.; Bertoni, M.; Bienert, S.; Studer, G.; Tauriello, G.; Gumienny, R.; Heer, F. T.; De Beer, T. A. P.; Rempfer, C.; Bordoli, L.; et al. SWISS-MODEL: Homology Modelling of Protein Structures and Complexes. *Nucleic Acids Res.* **2018**, *46*, W296–W303.
- (36) Süssmuth, R. D.; Mainz, A. Nonribosomal Peptide Synthesis-Principles and Prospects. *Angew. Chem., Int. Ed.* **2017**, *56*, 3770–3821
- (37) Wilson, D. J.; Aldrich, C. C. A Continuous Kinetic Assay for Adenylation Enzyme Activity and Inhibition. *Anal. Biochem.* **2010**, 404, 56–63.
- (38) Ronan, J. L.; Kadi, N.; McMahon, S. A.; Naismith, J. H.; Alkhalaf, L. M.; Challis, G. L. Desferrioxamine Biosynthesis: Diverse Hydroxamate Assembly by Substrate-Tolerant Acyl Transferase DesC. *Philos. Trans. R. Soc. London, Ser. B* **2018**, 373, W597–W600.
- (39) Beck, Z. Q.; Aldrich, C. C.; Magarvey, N. A.; Georg, G. I.; Sherman, D. H. Chemoenzymatic Synthesis of Cryptophycin/Arenastatin Natural Products. *Biochemistry* **2005**, *44*, 13457–13466.
- (40) Gaudelli, N. M.; Townsend, C. A. Epimerization and Substrate Gating by a TE Domain in β -Lactam Antibiotic Biosynthesis. *Nat. Chem. Biol.* **2014**, *10*, 251–258.
- (41) Hoyer, K. M.; Mahlert, C.; Marahiel, M. A. The Iterative Gramicidin s Thioesterase Catalyzes Peptide Ligation and Cyclization. *Chem. Biol.* **2007**, *14*, 13–22.
- (42) Boddy, C. N.; Schneider, T. L.; Hotta, K.; Walsh, C. T.; Khosla, C. Epothilone C Macrolactonization and Hydrolysis Are Catalyzed by the Isolated Thioesterase Domain of Epothilone Polyketide Synthase. *J. Am. Chem. Soc.* **2003**, *125*, 3428–3429.
- (43) Schaffer, J. E.; Reck, M. R.; Prasad, N. K.; Wencewicz, T. A. β -Lactone Formation during Product Release from a Nonribosomal Peptide Synthetase. *Nat. Chem. Biol.* **2017**, *13*, 737–744.
- (44) Lin, H.; Thayer, D. A.; Wong, C. H.; Walsh, C. T. Macrolactamization of Glycosylated Peptide Thioesters by the Thioesterase Domain of Tyrocidine Synthetase. *Chem. Biol.* **2004**, *11*, 1635–1642.
- (45) Akey, D. L.; Kittendorf, J. D.; Giraldes, J. W.; Fecik, R. A.; Sherman, D. H.; Smith, J. L. Structural Basis for Macrolactonization by the Pikromycin Thioesterase. *Nat. Chem. Biol.* **2006**, *2*, 537–542. (46) Nakamura, H.; Wang, J. X.; Balskus, E. P. Assembly Line Termination in Cylindrocyclophane Biosynthesis: Discovery of an

- Editing Type II Thioesterase Domain in a Type I Polyketide Synthase. Chem. Sci. 2015, 6, 3816–3822.
- (47) Ohlemacher, S. I.; Xu, Y.; Kober, D. L.; Malik, M.; Nix, J. C.; Brett, T. J.; Henderson, J. P. YbtT Is a Low-Specificity Type II Thioesterase That Maintains Production of the Metallophore Yersiniabactin in Pathogenic Enterobacteria. *J. Biol. Chem.* **2018**, 293, 19572–19585.
- (48) Drake, E. J.; Gulick, A. M. Structural Characterization and High-Throughput Screening of Inhibitors of PvdQ, an NTN Hydrolase Involved in Pyoverdine Synthesis. *ACS Chem. Biol.* **2011**, 6, 1277–1286.
- (49) Yeterian, E.; Martin, L. W.; Guillon, L.; Journet, L.; Lamont, I. L.; Schalk, I. J. Synthesis of the Siderophore Pyoverdine in *Pseudomonas aeruginosa* Involves a Periplasmic Maturation. *Amino Acids* **2010**, *38*, 1447–1459.
- (50) Loomis, L. D.; Raymond, K. N. Solution Equilibria of Enterobactin and Metal-Enterobactin Complexes. *Inorg. Chem.* **1991**, *30*, 906–911.
- (51) Lin, H.; Fischbach, M. A.; Liu, D. R.; Walsh, C. T. In Vitro Characterization of Salmochelin and Enterobactin Trilactone Hydrolases IroD, IroE, and Fes. *J. Am. Chem. Soc.* **2005**, *127*, 11075–11084.
- (52) Raines, D. J.; Moroz, O. V.; Blagova, E. V.; Turkenburg, J. P.; Wilson, K. S.; Duhme-Klair, A. K. Bacteria in an Intense Competition for Iron: Key Component of the Campylobacter Jejuni Iron Uptake System Scavenges Enterobactin Hydrolysis Product. *Proc. Natl. Acad. Sci. U.S.A.* 2016, 113, 5850–5855.
- (53) Okujo, N.; Saito, M.; Yamamoto, S.; Yoshida, T.; Miyoshi, S.; Shinoda, S. Structure of Vulnibactin, a New Polyamine-Containing Siderophore from Vibrio Vulnificus. *Biometals* **1994**, *7*, 109–116.
- (54) Kaplan, A. R.; Musaev, D. G.; Wuest, W. M. Pyochelin Biosynthetic Metabolites Bind Iron and Promote Growth in Pseudomonads Demonstrating Siderophore-like Activity. ACS Infect. Dis. 2021, 7, 544–551.
- (55) Ohlemacher, S. I.; Giblin, D. E.; D'Avignon, D. A.; Stapleton, A. E.; Trautner, B. W.; Henderson, J. P. Enterobacteria Secrete an Inhibitor of Pseudomonas Virulence during Clinical Bacteriuria. *J. Clin. Invest.* **2017**, *127*, 4018–4030.
- (56) Marshall, C. G.; Hillson, N. J.; Walsh, C. T. Catalytic Mapping of the Vibriobactin Biosynthetic Enzyme VibF. *Biochemistry* **2002**, *41*, 244–250.
- (57) Marshall, C. G.; Hillson, N. J.; Walsh, C. T. Catalytic Mapping of the Vibriobactin Biosynthetic Enzyme VibF. *Biochemistry* **2002**, *41*, 244–250.
- (58) Hillson, N. J.; Balibar, C. J.; Walsh, C. T. Catalytically Inactive Condensation Domain C1 Is Responsible for the Dimerization of the VibF Subunit of Vibriobactin Synthetase. *Biochemistry* **2004**, *43*, 11344–11351.
- (59) Balibar, C. J.; Walsh, C. T. From Thioesters to Amides and Back: Condensation Domain Reversibility in the Biosynthesis of Vibriobactin. *ChemBioChem* **2008**, *9*, 42–45.
- (60) Shapiro, J. A.; Wencewicz, T. A. Structure-Function Studies of Acinetobactin Analogs. *Metallomics* **2017**, *9*, 463–470.
- (61) Suzuki, K.; Tanabe, T.; Moon, Y.-H.; Funahashi, T.; Nakao, H.; Narimatsu, S.; Yamamoto, S. Identification and Transcriptional Organization of Aerobactin Transport and Biosynthesis Cluster Genes of Vibrio Hollisae. *Res. Microbiol.* **2006**, *157*, 730–740.
- (62) Lemoine, F.; Correia, D.; Lefort, V.; Doppelt-Azeroual, O.; Mareuil, F.; Cohen-Boulakia, S.; Gascuel, O. NGPhylogeny.Fr: New Generation Phylogenetic Services for Non-Specialists. *Nucleic Acids Res.* **2019**, *47*, W260–W265.
- (63) Letunic, I.; Bork, P. Interactive Tree Of Life (ITOL): An Online Tool for Phylogenetic Tree Display and Annotation. *Bioinformatics* **2007**, 23, 127–128.
- (64) McWilliam, H.; Li, W.; Uludag, M.; Squizzato, S.; Park, Y. M.; Buso, N.; Cowley, A. P.; Lopez, R. Analysis Tool Web Services from the EMBL-EBI. *Nucleic Acids Res.* **2013**, *41*, W597–W600.
- (65) Robert, X.; Gouet, P. Deciphering Key Features in Protein Structures with the New ENDscript Server. *Nucleic Acids Res.* **2014**, 42, W320–W324.

(66) Wong, C. H.; Gordon, J.; Cooney, C. L.; Whitesides, G. M. Regeneration of NAD(P)H Using Glucose 6-Sulfate and Glucose-6-Phosphate Dehydrogenase. *J. Org. Chem.* **1981**, *46*, 4676–4679.